Voxel-wise Comparison of Quantitative Perfusion Imaging Using Pulsed and Continuous Arterial Spin Labeling Techniques at 3T

W-M. Luh[1], S. L. Talagala[2], P. A. Bandettini[3]

[1]National Institutes of Health, Bethesda, MD, United States, [2]NINDS, National Institutes of Health, Bethesda, MD, United States, [3]FMRIF/NIMH, National Institutes of Health, Bethesda, MD, United States

Introduction

Arterial spin labeling (ASL) techniques can be used to measure perfusion noninvasively with continuous or pulsed labeling. Continuous ASL (CASL) creates the tagging blood in finite space and utilizes time for building up the width of the tag whereas pulsed ASL (PASL) inverts the spins in a finite time period and relies on available space to create the tag. Both techniques allow for quantitative estimation of cerebral blood flow (CBF) by incorporating post-labeling delay. CASL techniques are more limited by magnetization transfer and RF power deposition and PASL techniques are more limited by slice profile issues and available tagging space if head coil is used. Due to longer T1 at high field strength, ASL techniques benefit higher SNR although it may hinder CASL performance. However the limitation on CASL can be substantially reduced with a separate local labeling coil. A comparison study of both techniques was previous performed on 1.5T using amplitude-modulated CASL and QUIPSS II (1) but voxel-wise comparison studies are lacking. Here we performed a direct voxel-wise comparison study with QUIPSS II (2) and CASL with a separate labeling coil (3) at 3T with the additionally acquired T1 maps for tissue identification.

Methods

A Nova Medical volume transmit/receive head coil was used for image excitation and acquisition with normal volunteers on a 3T GE Signa MRI scanner. For CASL, a surface labeling coil was placed on the neck to achieve inversion of flowing spins in the carotid and vertebral arteries(3). The labeling period was 3 sec with 1.7 W RF power applied to the labeling coil at an offset of ~20 kHz in the presence of a 0.3 G/cm gradient along the superior-inferior direction. A labeling efficiency of ~75% was measured in the carotid artery 3.2 cm above the labeling coil. A post-labeling delay of 1.5 sec was used with a TR of 5 sec. The control images were acquired with the reversal of the gradient polarity. A total of 100 pairs of tagged and control images was obtained with single-shot gradient-echo EPI with TE/TR=25/2000 ms and FOV=24 cm with five 7 mm skip 1mm axial slices and 3.75x3.75 mm in-plane resolution. For the pulsed ASL, PICORE QUIPSS II (2) was used with TI1/TI2=700/1500 ms and 10 cm tagging slab with 1 cm gap to the imaging slices. A total of 250 pairs of tagged/control EPI images were acquired with the QUIPSS II saturation pulses applied twice in a row to achieve similar saturation in the tagging area as in Q2TIPS (4). ASL images were pair-wise subtracted and averaged to obtain perfusion images. The absolute CBF values were calculated with a general kinetic model (1) with an assumed T1 of blood of 1500 ms. The time period Tex from the labeling site to the tissue site where the blood spins exchange into tissues was assumed to be 1400 ms for CASL and 900 ms for PASL. Blood magnetization was estimated from the WM signal as described in (2). In addition, TI-stepping inversion recovery EPI images were obtained for the same slices with 16 TI values from 50 ms to 5999 ms varying logarithmically for a TR of 6 sec. The T1 value of each voxel was also used in the kinetic model for estimating ASL CBF values. All raw images were inspected visually in cine mode for alignment and were registered for bulk motion correction if applicable.

Results

Figure1 shows the PASL CBF (top), CASL CBF (middle), and T1 (bottom) images. The first PASL slice shows an overall higher intensity than the rest of slices due to known imperfect static tissue signal subtraction (5). Both PASL and CASL images show very similar contrast. Figure 2 shows the scatter plots of both perfusion images of the second slice vs. T1. In the T1 range of WM/GM, similar patterns are observed with an approximately linear relationship with T1 as reported earlier (6). The correlation coefficients (CC) between PASL and CASL data in the each slice as well as in the gray matter (GM) and WM ROIs (similar in size selected by T1 values) are shown in Table 1. The data from both techniques are highly correlated. Figure 3 shows the example scatter plot of the second slice between PASL and CASL data. CASL shows higher CBF values than PASL in voxels with high flow values. All slices exhibit similar patterns in the scatter plots.

Discussion

CASL and PASL data are highly correlated although PASL shows a trend of decreasing CBF toward distal slices probably due to imperfect slice profile effects. Although the correlations are high between both techniques, the estimated CBF values have different dependency in assumed parameters such as Tex and tissue T1. Although the T1 values from T1 maps were used for the tissue T1, for GM tissue the partial voluming with CSF and and WM will cause overestimation and underestimation of CBF, respectively. The Tex used is assumed for GM and will be longer for WM and for more distal slices. Both sensitivity to error in Tex and tissue T1 are higher for CASL than PASL especially for WM since for typical setting CASL is operating in the fully-exchange regime for GM and PASL is in the partial-exchange regime.

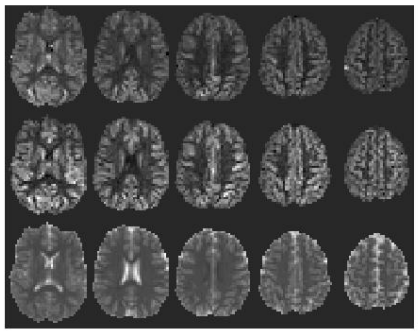

Figure 1. PASL CBF (top), CASL CBF(middle), and T1 (bottom) images.

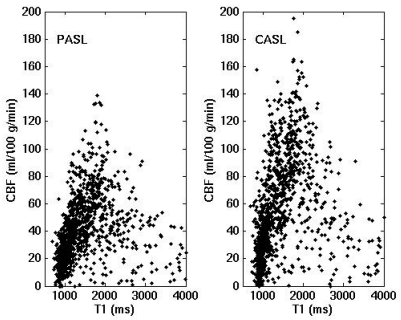

Figure 2. Scatter plot of CBF vs. T1 from voxels of the second slice.

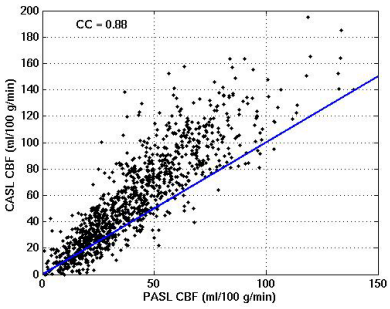

Figure 3. Scatter plot of PASL vs. CASL CBF from voxels of the second slice with the linear regression line (CC=0.88).

	1	2	3	4	5	All	PASL	CASL
volume	0.81	0.88	0.81	0.89	0.77	0.81	39.8	59.5
GM	0.82	0.84	0.81	0.88	0.85	0.74	47.1	75
WM	0.61	0.82	0.80	0.92	0.76	0.58	14.6	21.4

Table 1. Correlation coefficients of each slice and as a volume in the whole volume, GM, and WM ROIs, and the averaged CBF from both PASL and CASL in the whole volume, GM, and WM ROIs.

References

1. Wong et al., *MRM* 40: 348 (1998). 2. Wong et al., *MRM* 39: 702 (1998). 3. Talagala et al., *MRM* 52: 131 (2004). 4. Luh et al., *MRM* 41: 1246 (1999). 5. Frank et al., *MRM* 38: 558 (1997). 6. Luh et al., *MRM* 44: 137 (2000). 7. Ye et al., *MRM* 44: 450 (2000).